Development of a CO_2 Chemical Sensor for Downhole CO_2 Monitoring in Carbon Sequestration

Ning Liu

May 21, 2014

Petroleum Recovery Research Center
New Mexico Institute of Mining and Technology, Socorro, NM 87801
Phone: (575) 835-5739; Fax: (575) 835 6721; Email: ningliu@nmt.edu

Project goals and objectives

Objectives:

to develop a downhole CO_2 sensor that can monitor CO_2 plume migration in carbon sequestration. The proposed downhole CO_2 sensor can resist high pressure, temperature, and high salinity.

Phase I – To develop a metal-oxide pH electrode with good stability and to understand different factors' effects on the performance of the electrode.

Phase II – To develop a downhole CO_2 sensor and determine sensor performance under high pressure and high salinity.

Phase III – To evaluate the CO_2 sensor's response in CO_2/brine coreflooding tests, and to develop a data acquisition system for the developed CO_2 sensor.

Background

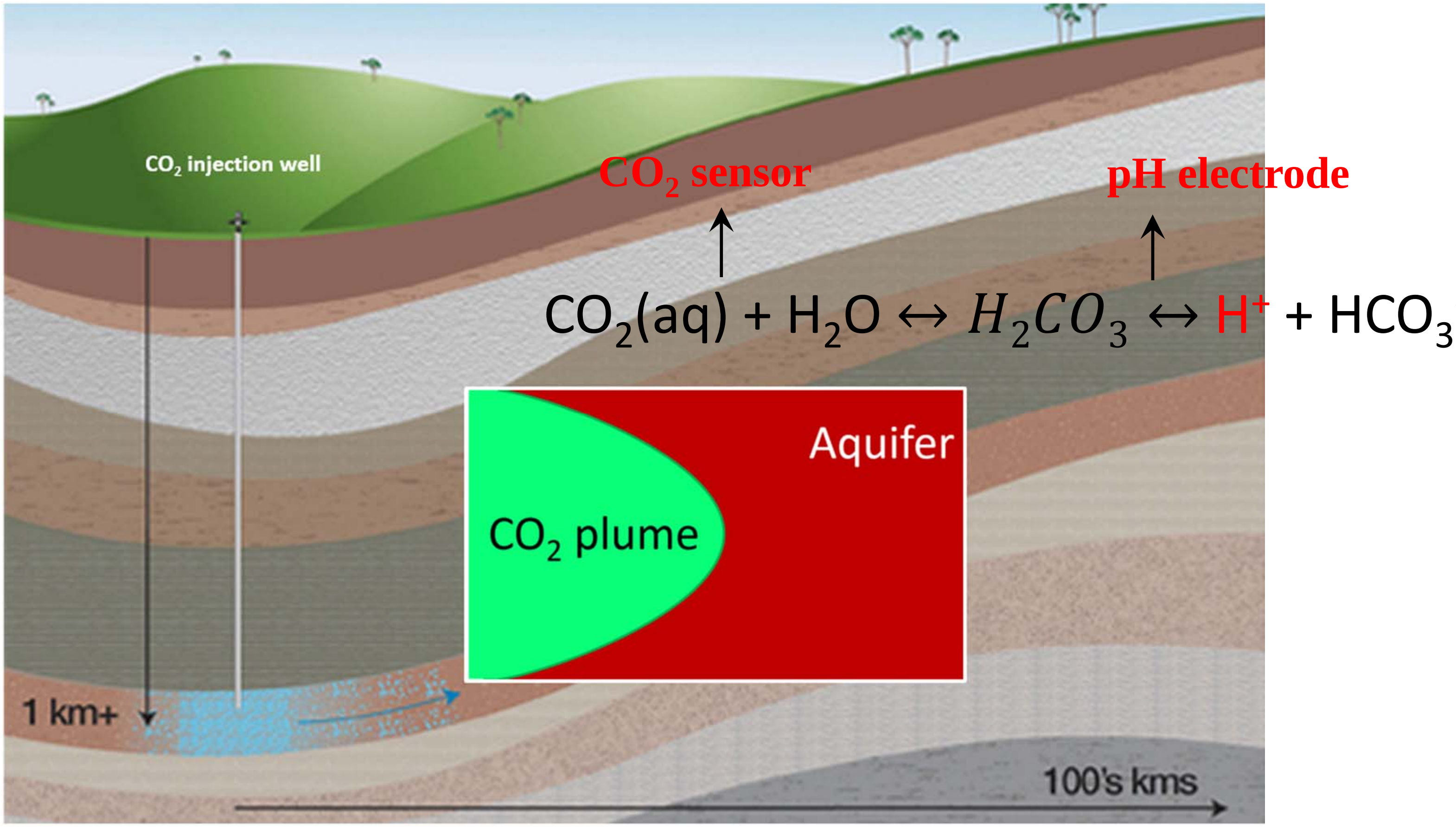

Figure 1. Schematic of CO_2 sequestration.

CO_2 chemical sensor design

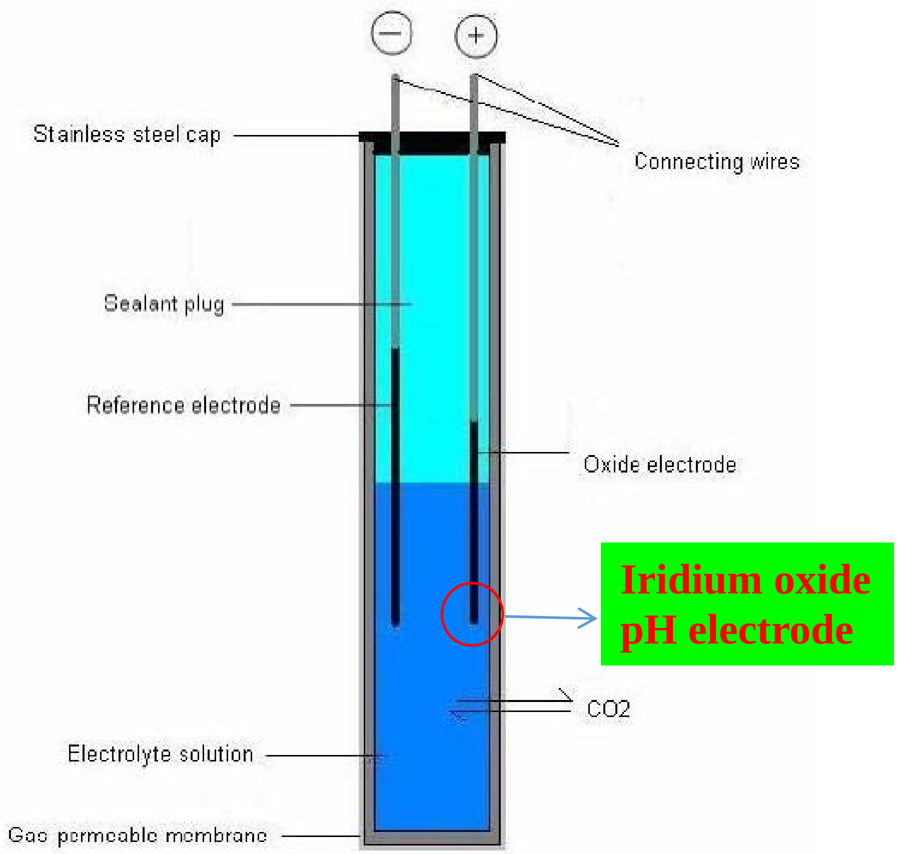

Figure 2. Schematic structure and picture of the fabricated CO_2 sensor.

Approach

Task 2.0 (1 year) Synthesize metal-oxide pH electrode and evaluate the electrode's performance.

- Subtask 2.1 Prepare the iridium oxide electrode
- Subtask 2.2 Test the performance of the prepared iridium oxide electrode
- Subtask 2.3 Effect of different ions, pressures, temperatures, and brine compositions on the performance of the electrode.
- Subtask 2.4 Investigate the stability and reproducibility of the IrO_x electrode.

Iridium oxide films preparation

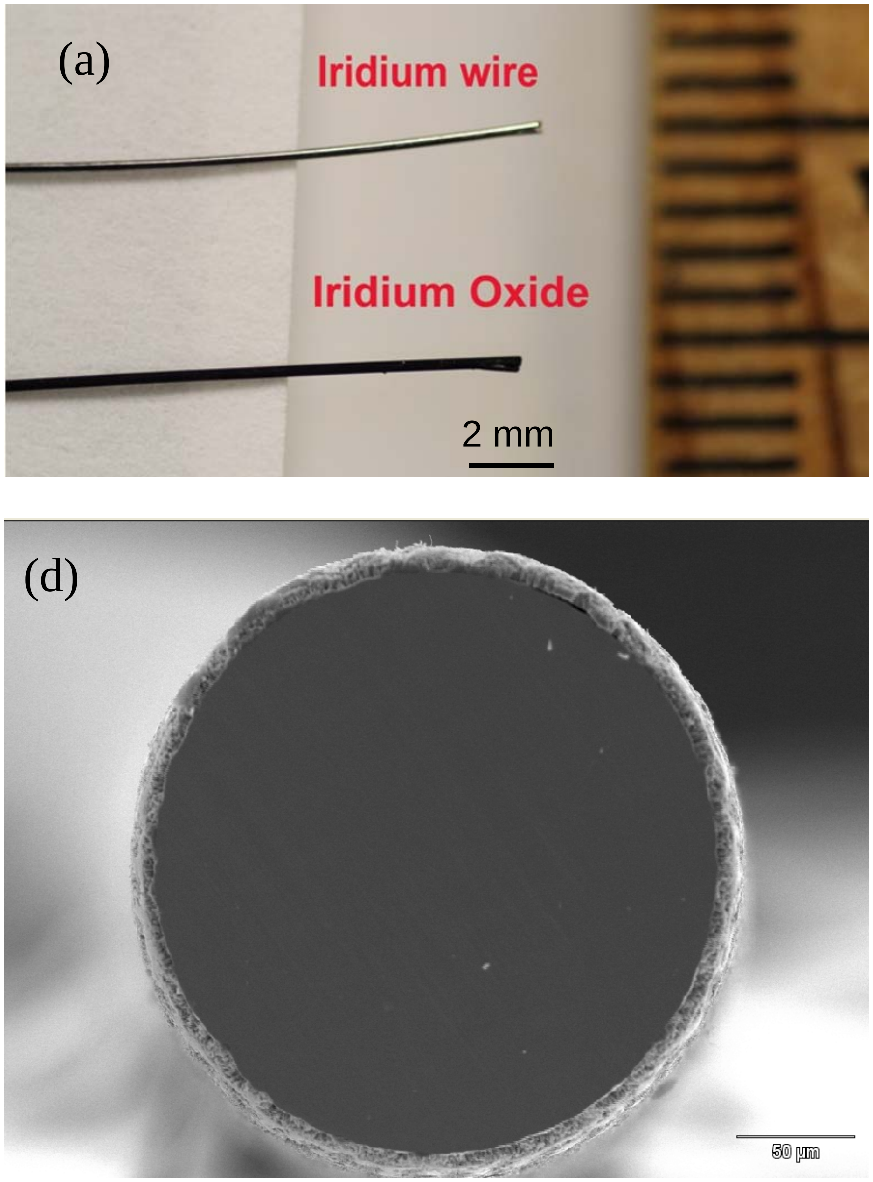

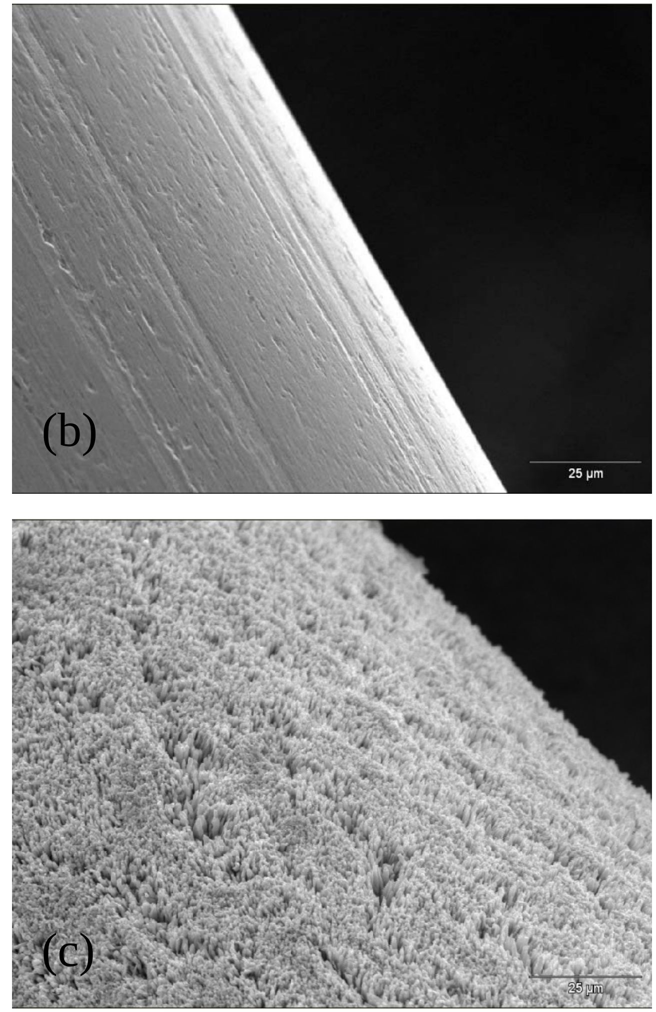

Figure 3. Micrograph of iridium oxide film prepared under 870° C and 5h: (a) overview of iridium wires before and after oxidation; (b) surface morphology of bare iridium wire; (c) surface morphology of iridium oxide; (d) Cross section of iridium oxide.

EDS, XPS

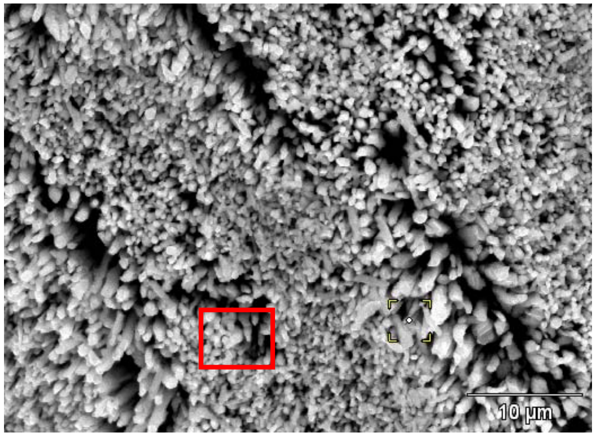

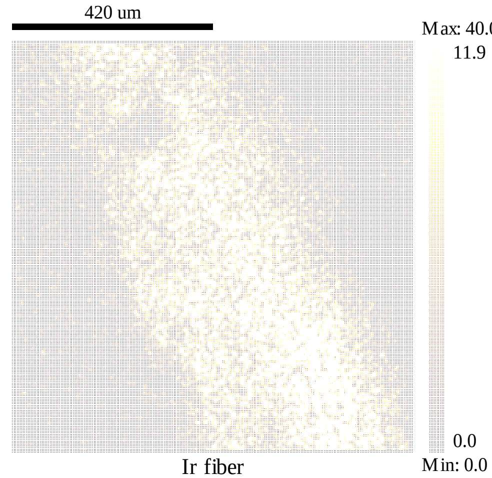

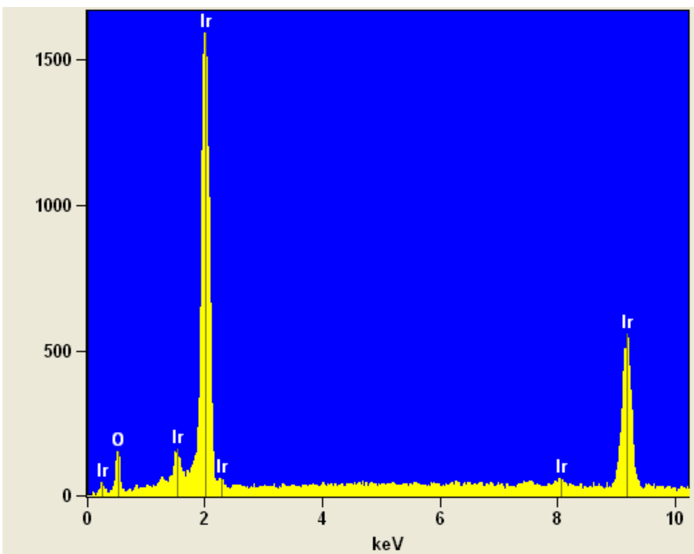

Figure 4. EDX analysis of iridium and iridium oxide film: (a) surface SEM image of IrOx film and (b) EDX analysis on the IrOx film from surface.

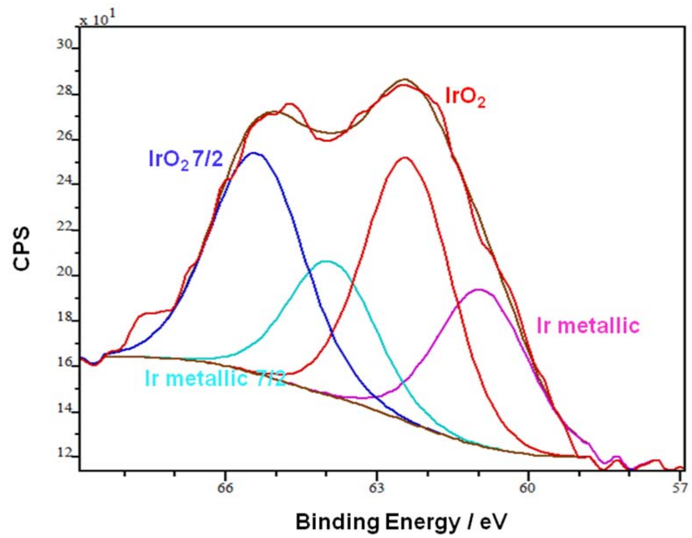

Figure 5. XPS spectra of iridium oxide fibers.

Temperature effects on iridium oxide film formation

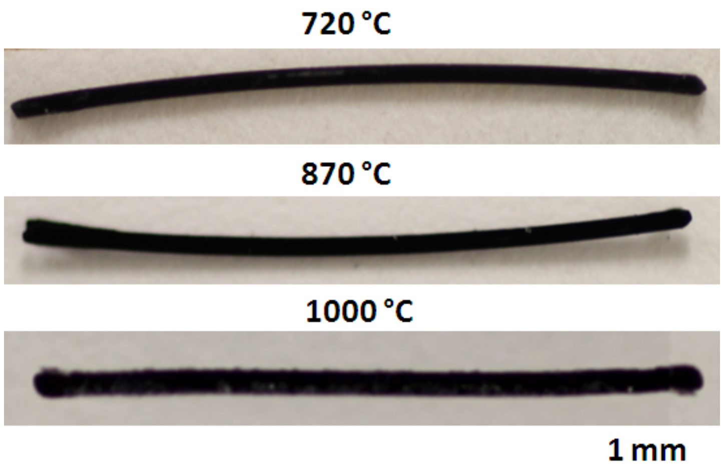

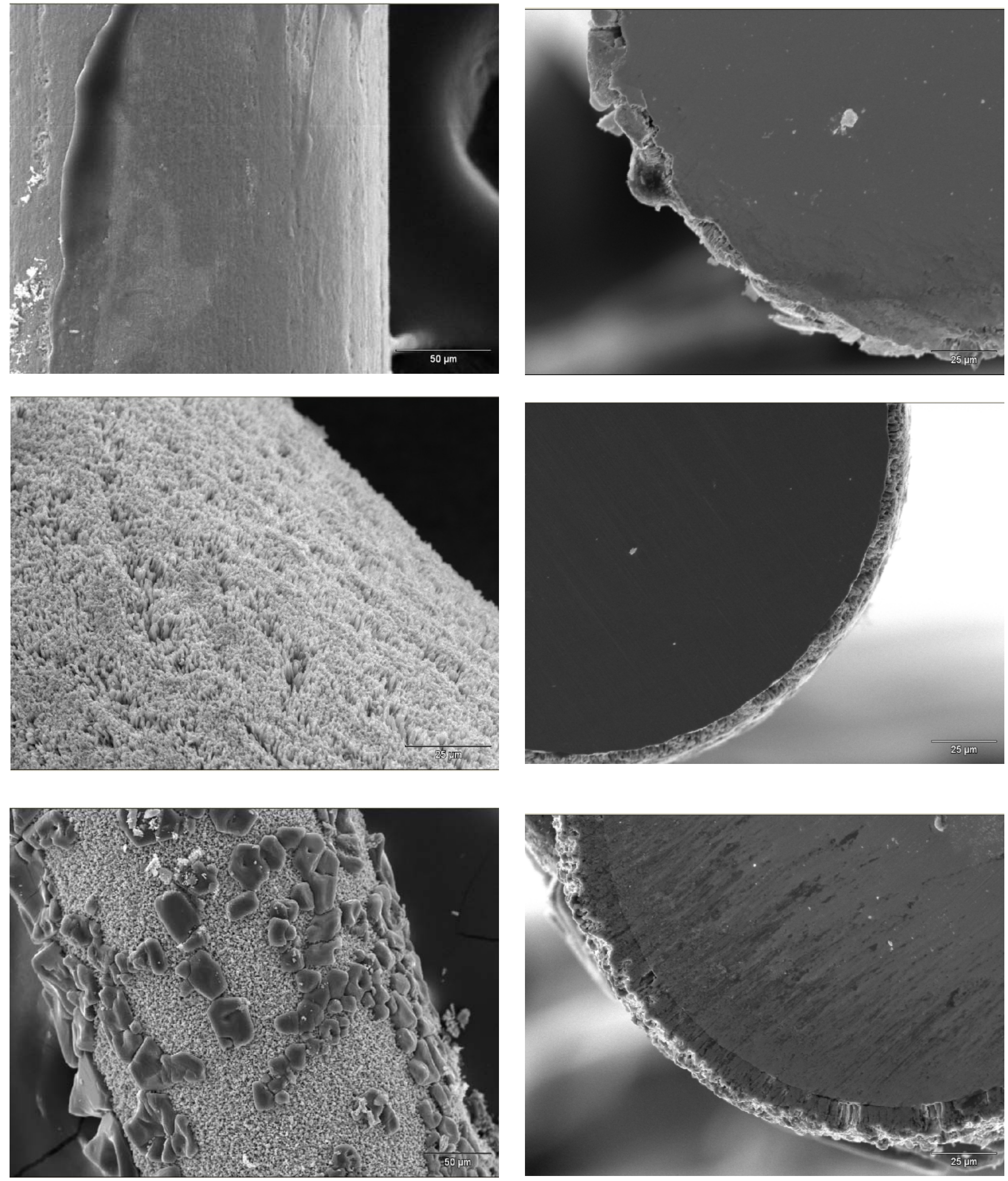

Figure 6. Micrograph of iridium oxide film prepared under different temperatures and fixed duration of 5h: (a) overview of iridium oxide wires under 720° C, 850° C and 1000 ° C, respectively; (b) surface and cross-section morphologies of iridium wires corresponding to the three specific temperatures.

Time effects on iridium film formation

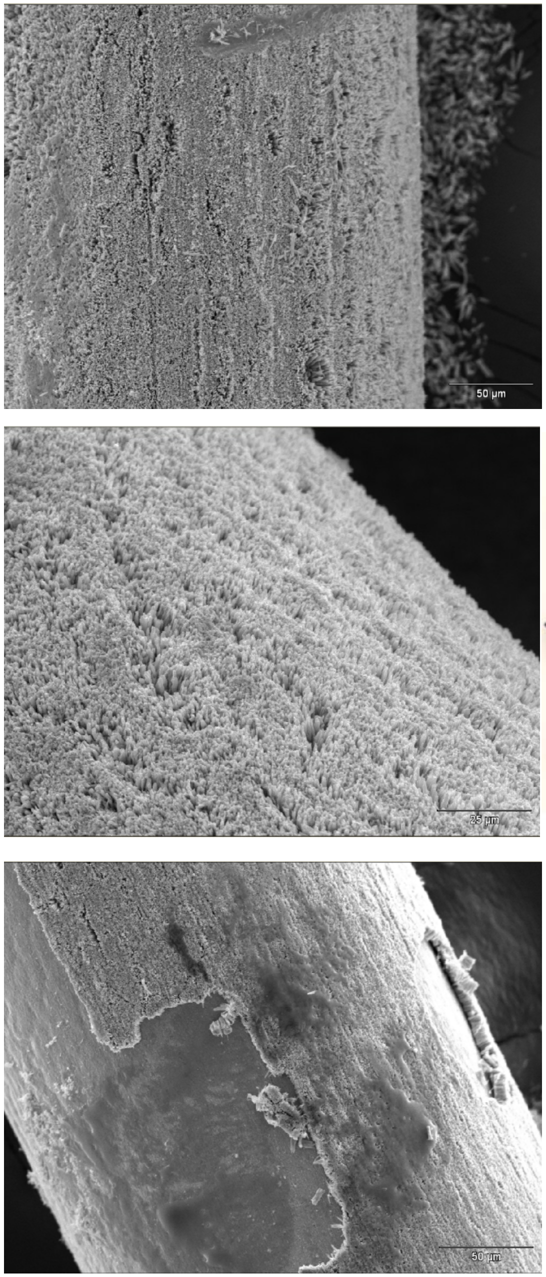

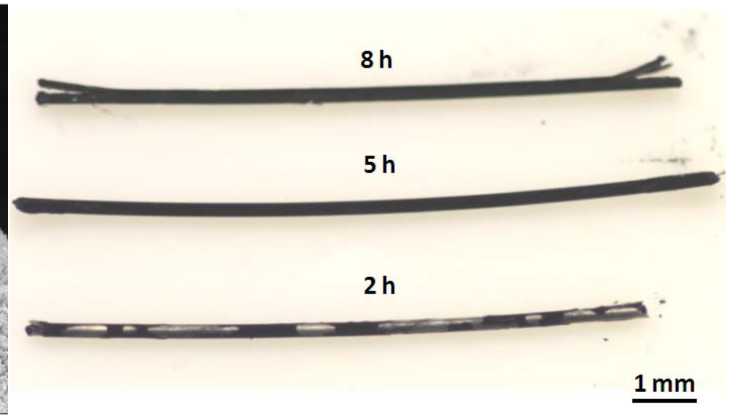

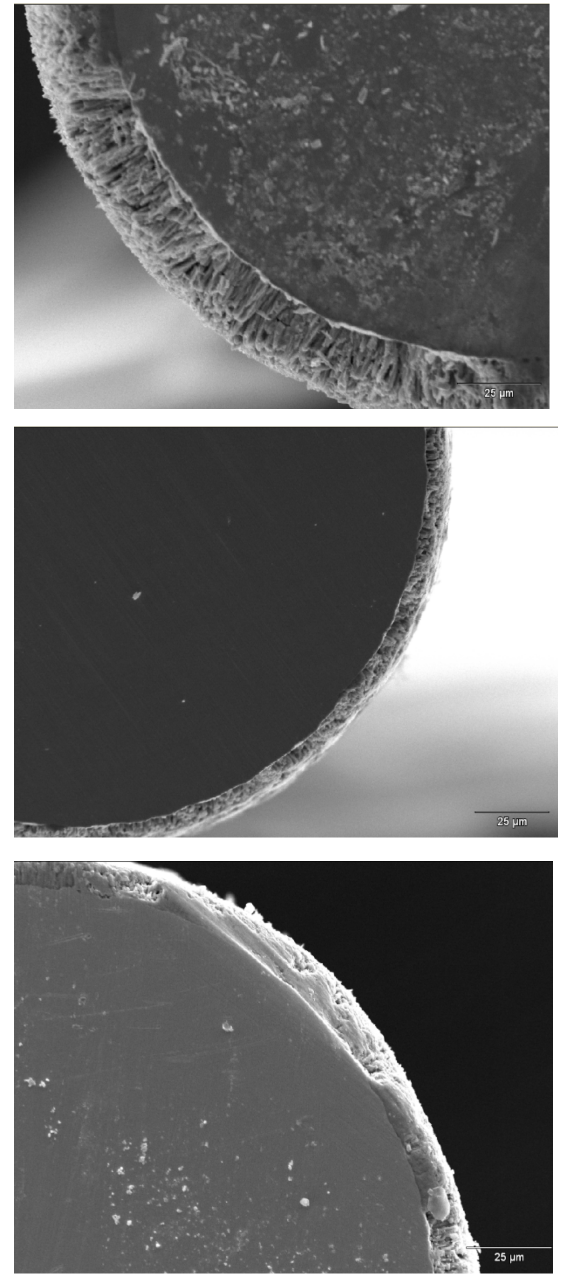

Figure 7. Micrograph of iridium oxide film prepared under different duration time and fixed temperature of 870° C : (a) overview of iridium oxide wires under 2 hours, 5 hours and 10 hours, respectively; (b) surface and cross-section morphologies of iridium wires corresponding to the three specific temperatures.

Potential measurement for Iridium oxide electrode

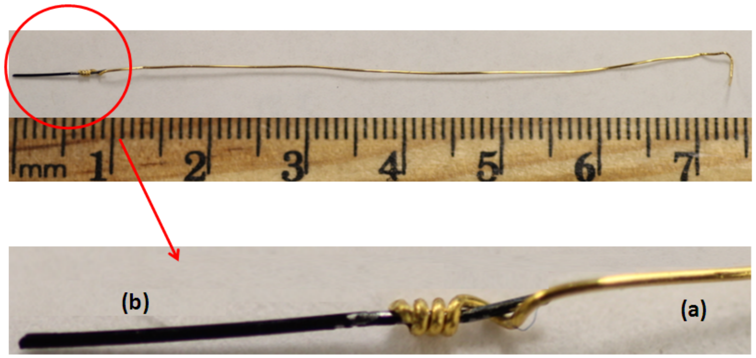

Figure 8. Iridium oxide pH electrode: (a) Oxidized Ir wire made from iridium wire with a diameter of 0.25 mm; (b) Au connecting wire with a diameter of 0.25 mm.

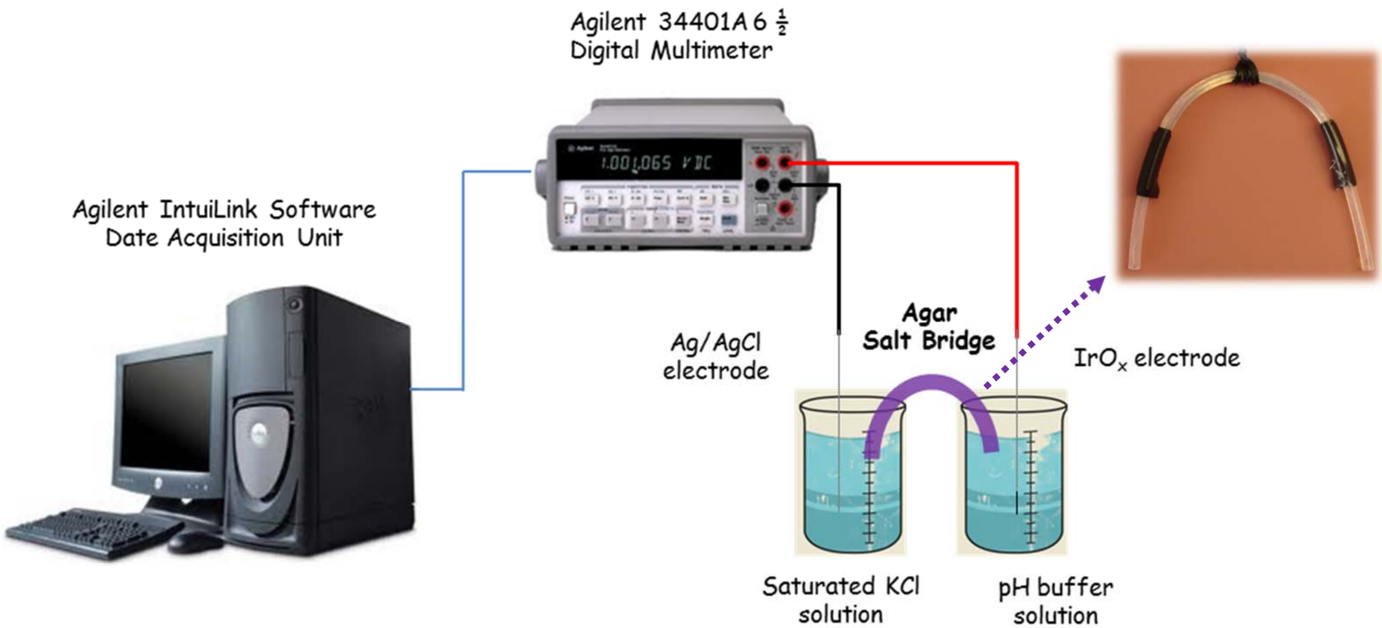

Figure 9. Schematic of pH response measurement apparatus.

Sensitivity of Iridium oxide electrode

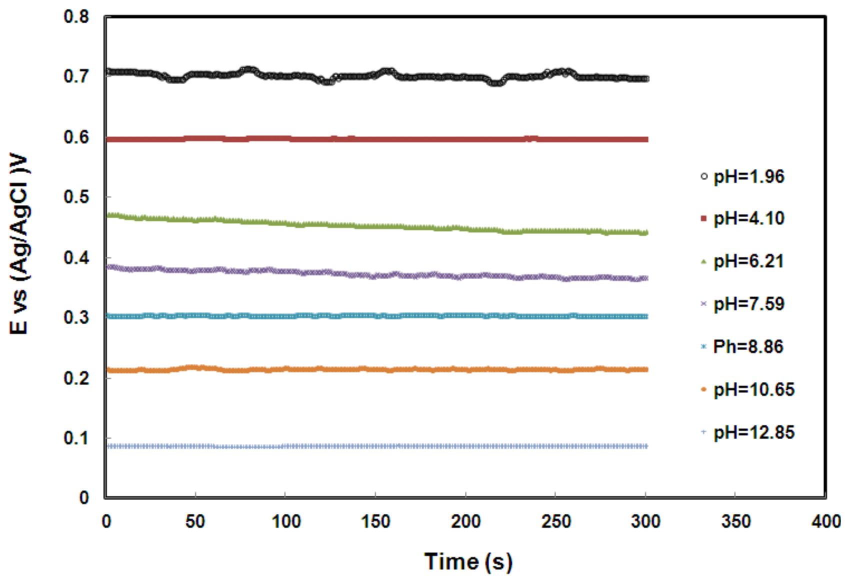

Figure 10. Potential responses in time of an IROF electrode in various buffer solutions.

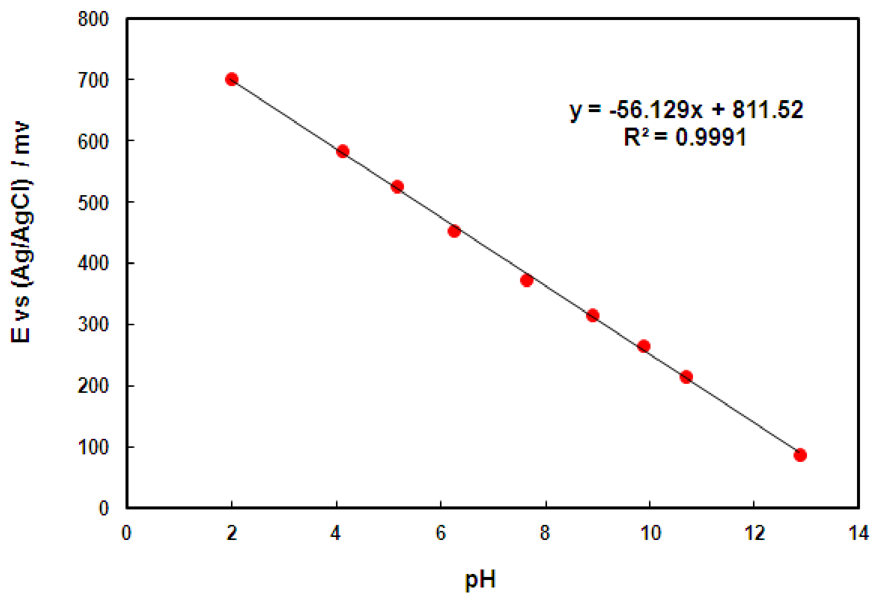

Figure 11. Potential of an IROF electrode as a function of pH.

Sensitivity of Iridium oxide electrode

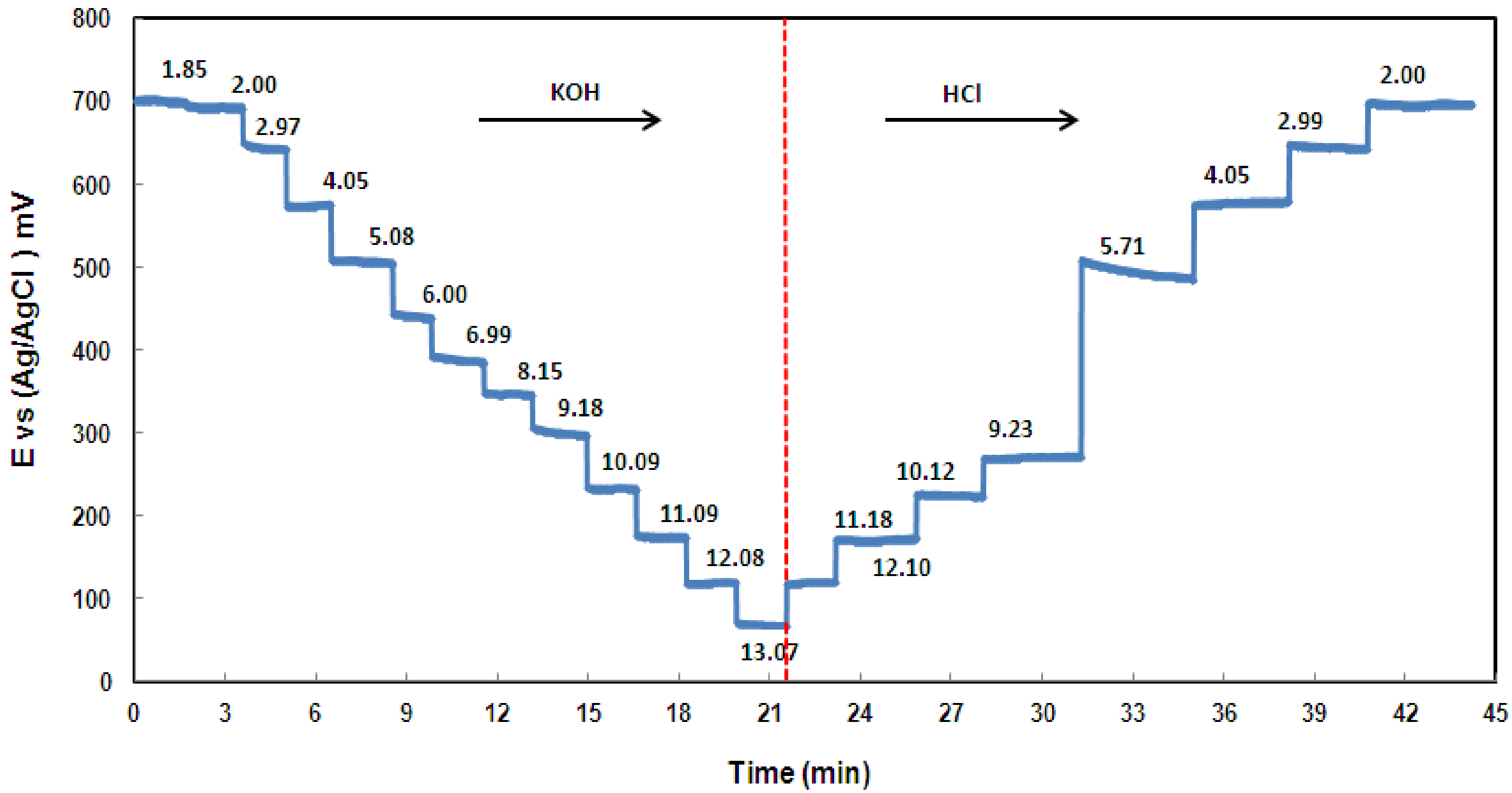

Figure 12. Potential response of an IROF electrode to pH changes in a serious of pH buffer solutions from pH 1.85 to 13.07.

Ions effects on IrO_2 electrode response

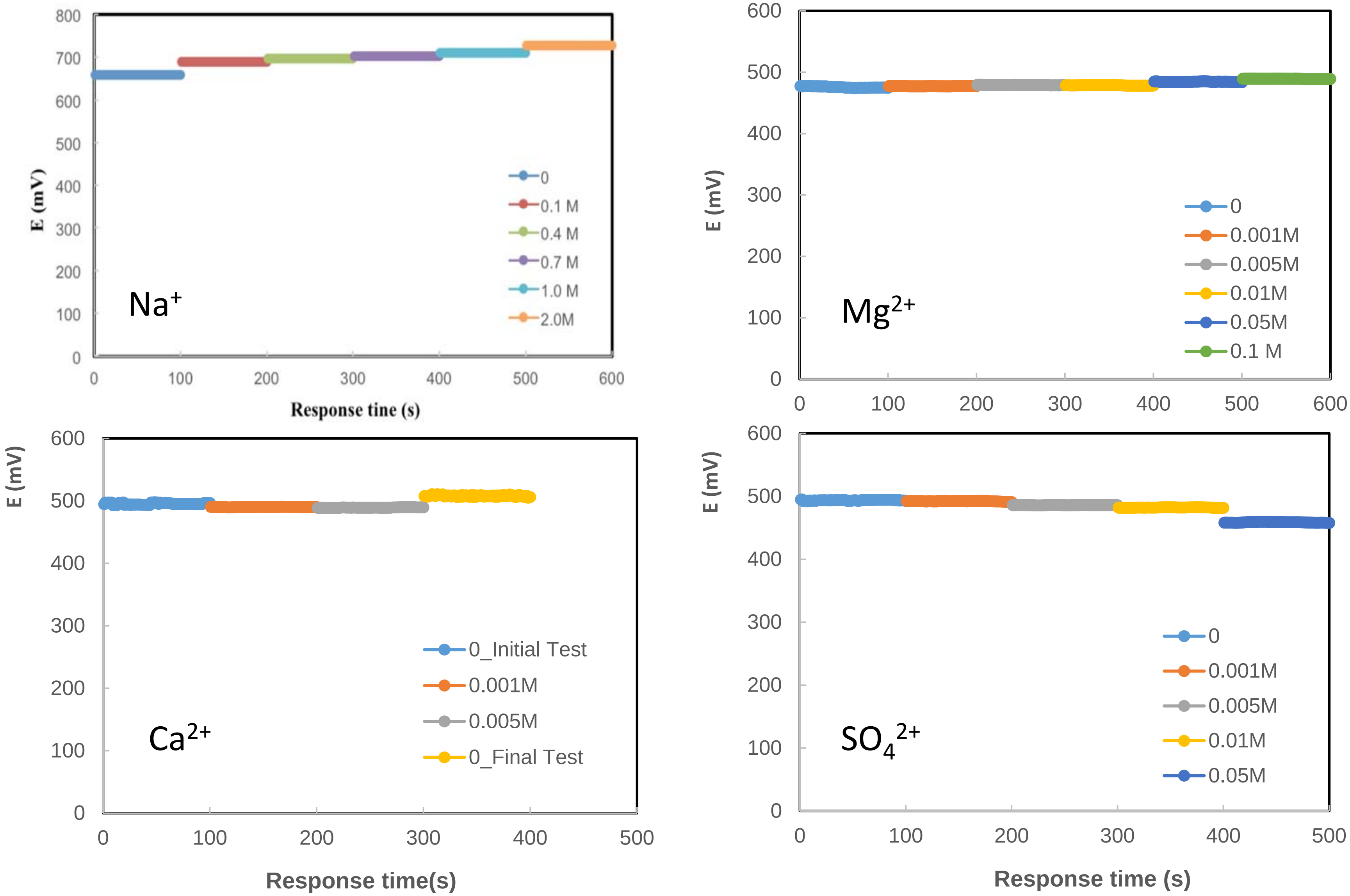

Figure 13.Na^+, Mg^{2+}, Ca^{2+} and SO_4^{2+} ions effects on the pH response of the IOx electrode.

Ions effects on IrO_2 electrode response

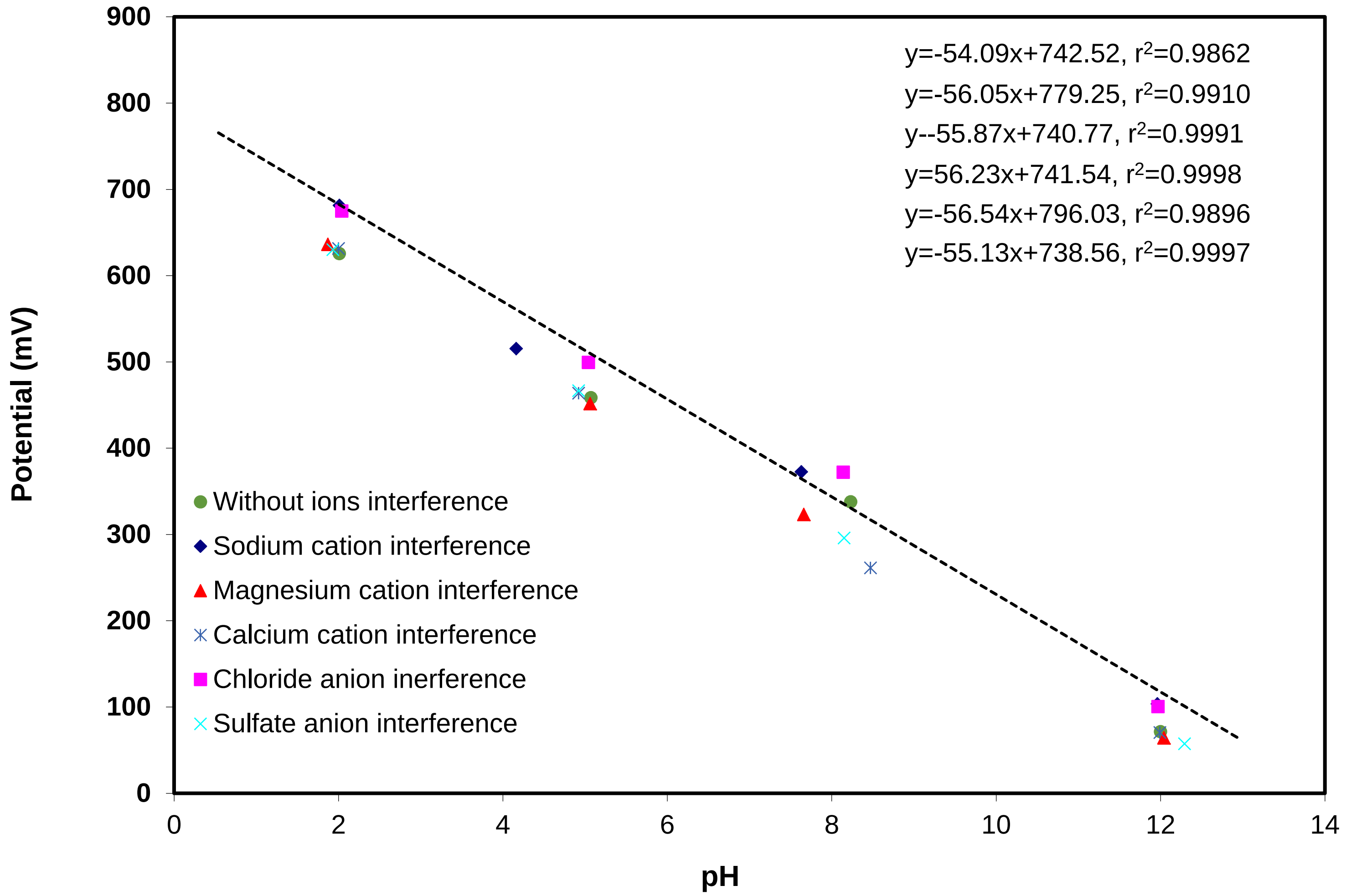

Figure 14. The effects of interference ions on the pH sensitivity.

Iridium oxide electrode performance in produced water

Table 1. Composition of produced water.

Ion (I)	Concentration (mg/L)
Na^+	11138
Mg^{2+}	78
Ca^{2+}	39
Cl^-	15299
SO_4^{2-}	33

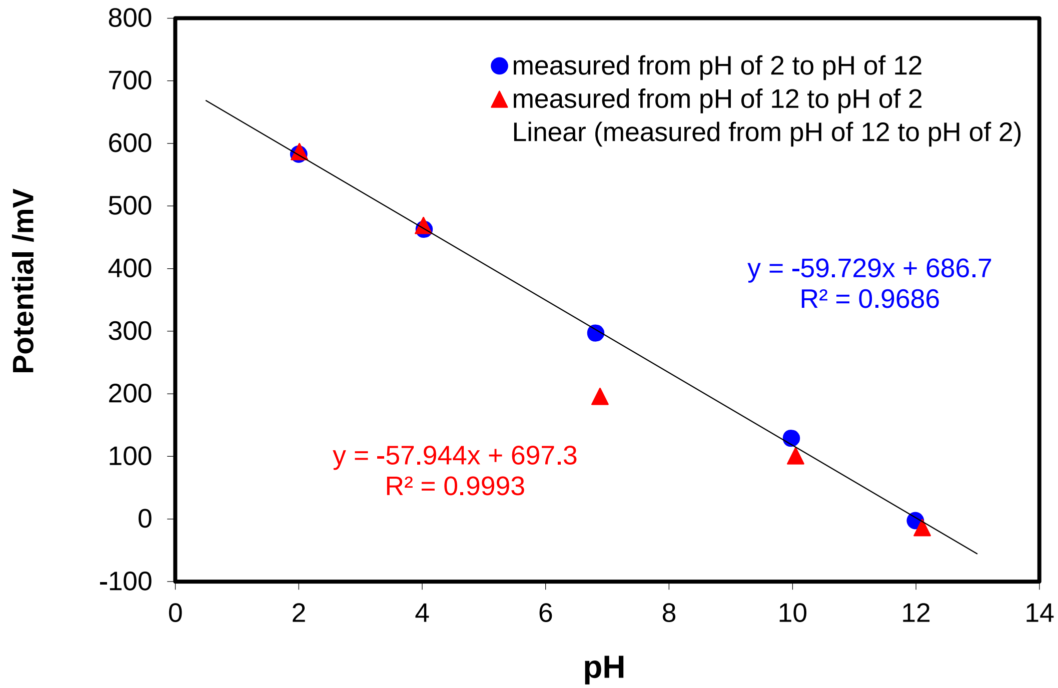

Figure 15. Reversibility tests of the prepared iridium oxide electrode in produced water.

Temperature effects on pH response

Nernstian equation:

$$2IrO_2+2H^++2e^-=Ir_2O_3+H_2O$$

$$E=E^0-2.303\frac{RT}{F}pH$$

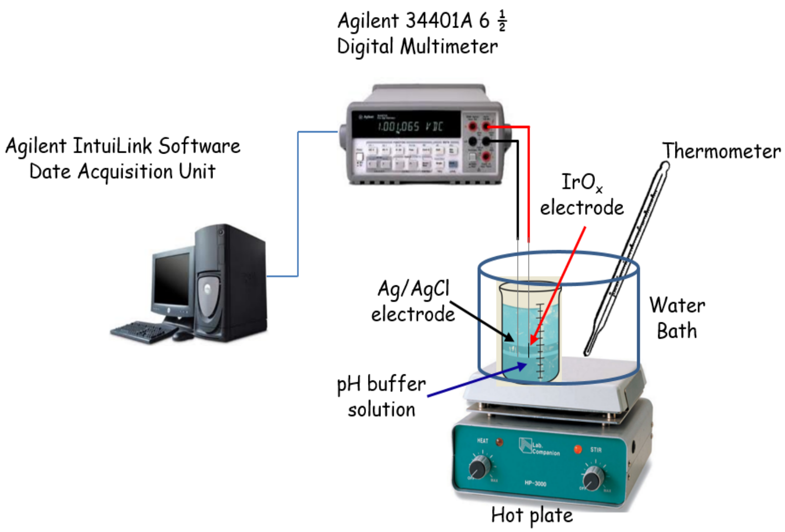

Figure 16. Schematic of pH response measurement apparatus.

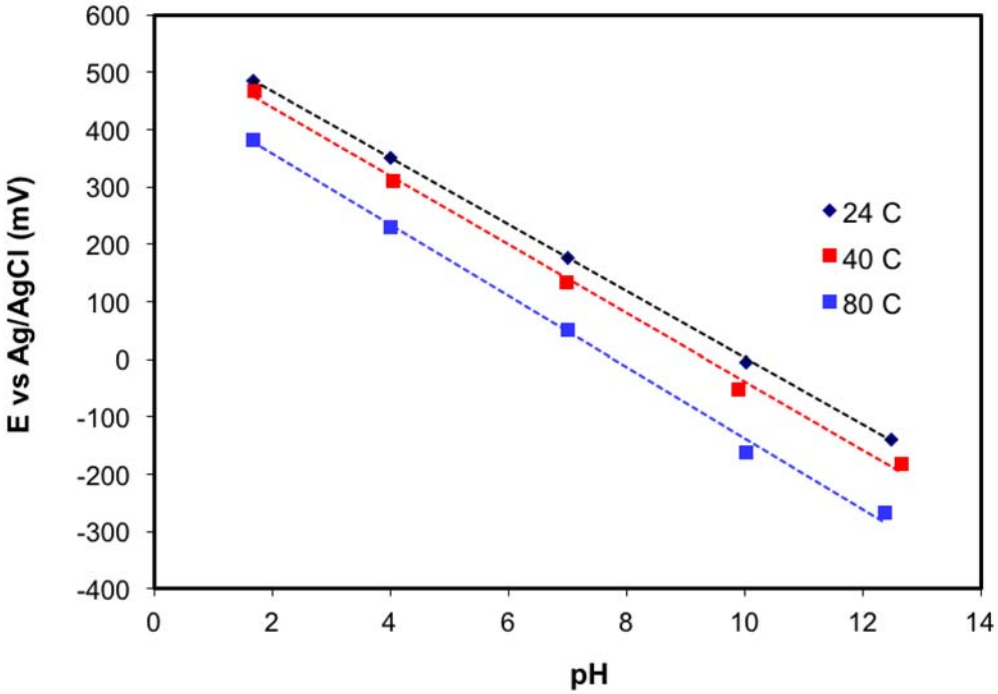

Figure 17. Temperature dependence of pH sensor.

Pressure effects on pH response

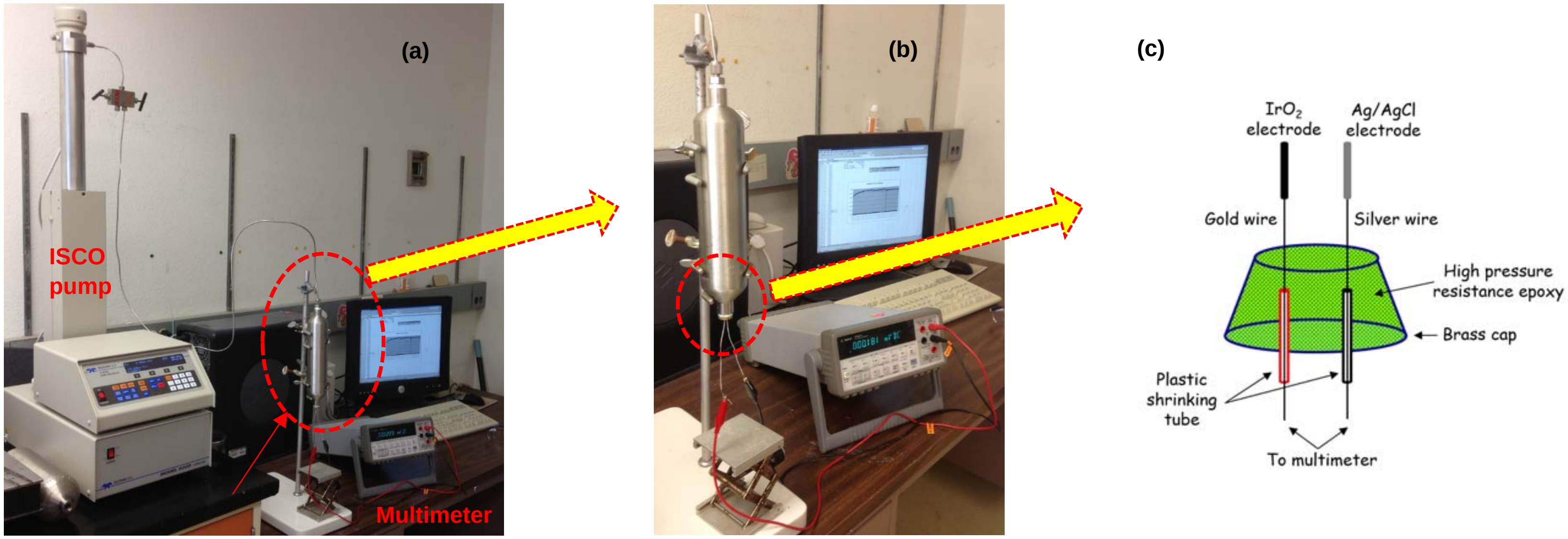

Figure 18. The apparatus for pH potential measurement at high pressures. (a) Apparatus overview; (b) pH sensor unit connected with multimeter and data acquisition system; (c) details of pH sensor unit.

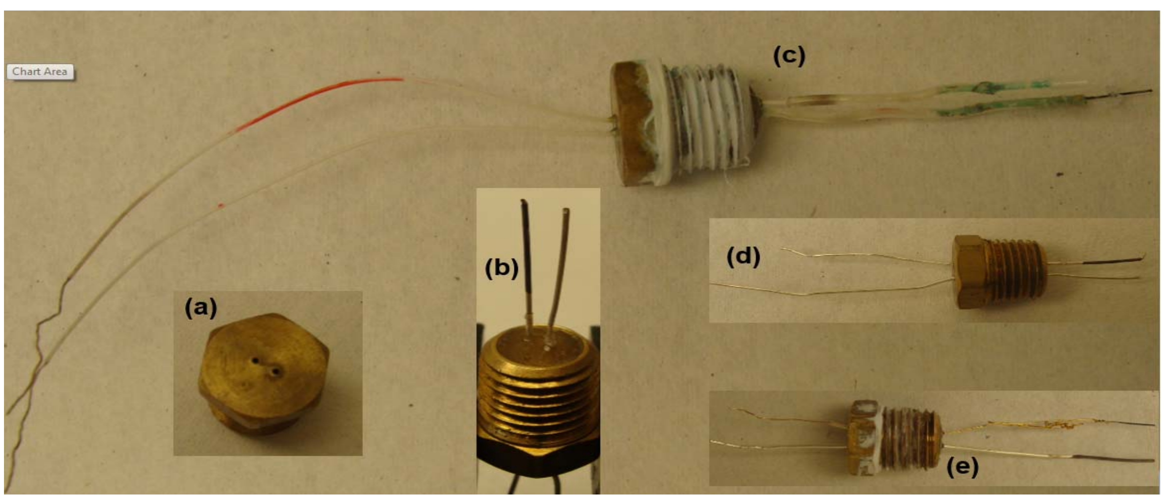

Figure 19. Photographs of pH sensor unit. (a) 1/4" brass cap with two small holes; (b) electrodes were stabilized with the epoxy in brass cap; (c, d, & e) pH sensor unit.

Pressure effects on pH response

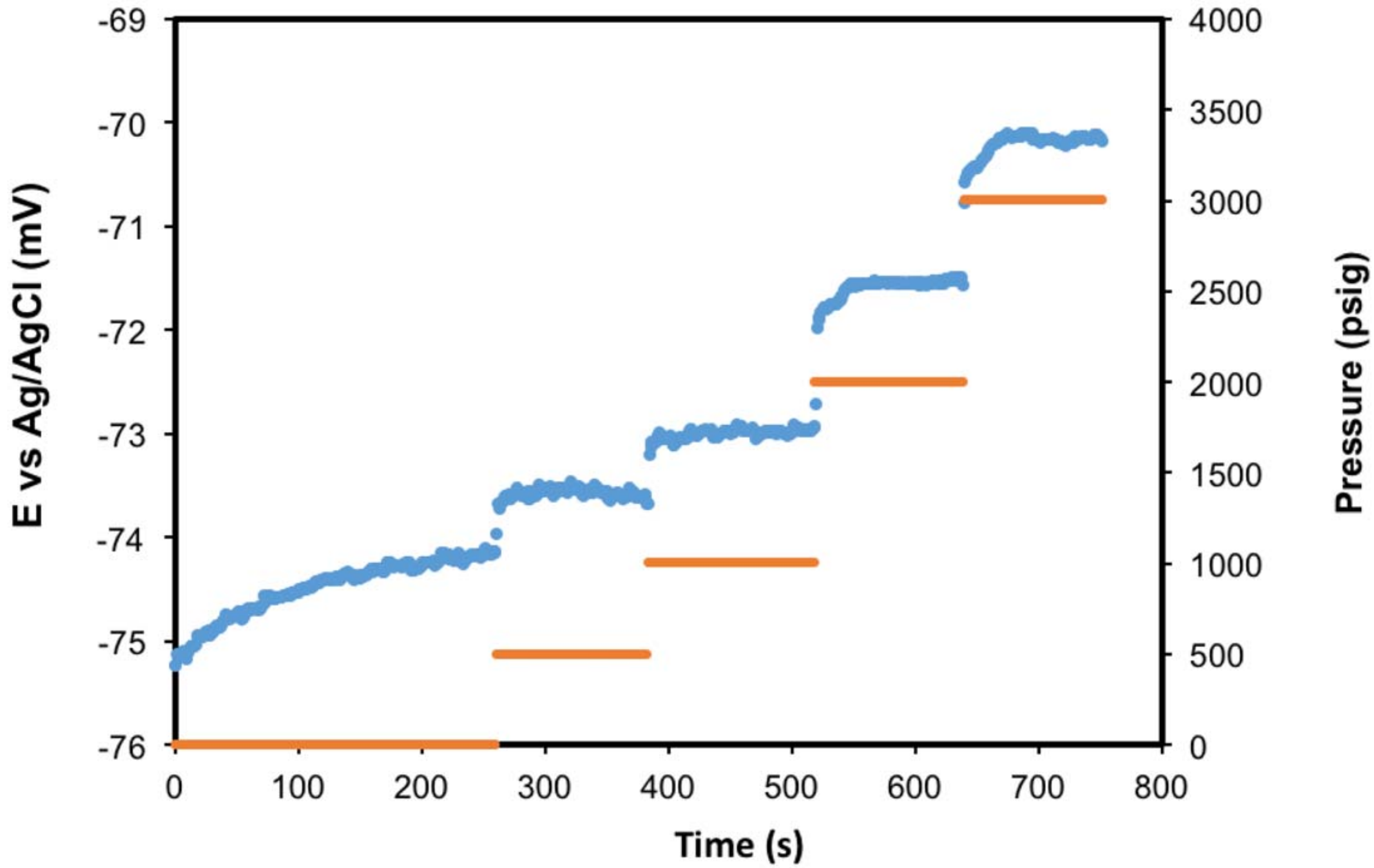

Figure 20. Potential and pressure response as a function of recording time.

Pressure effects on pH response

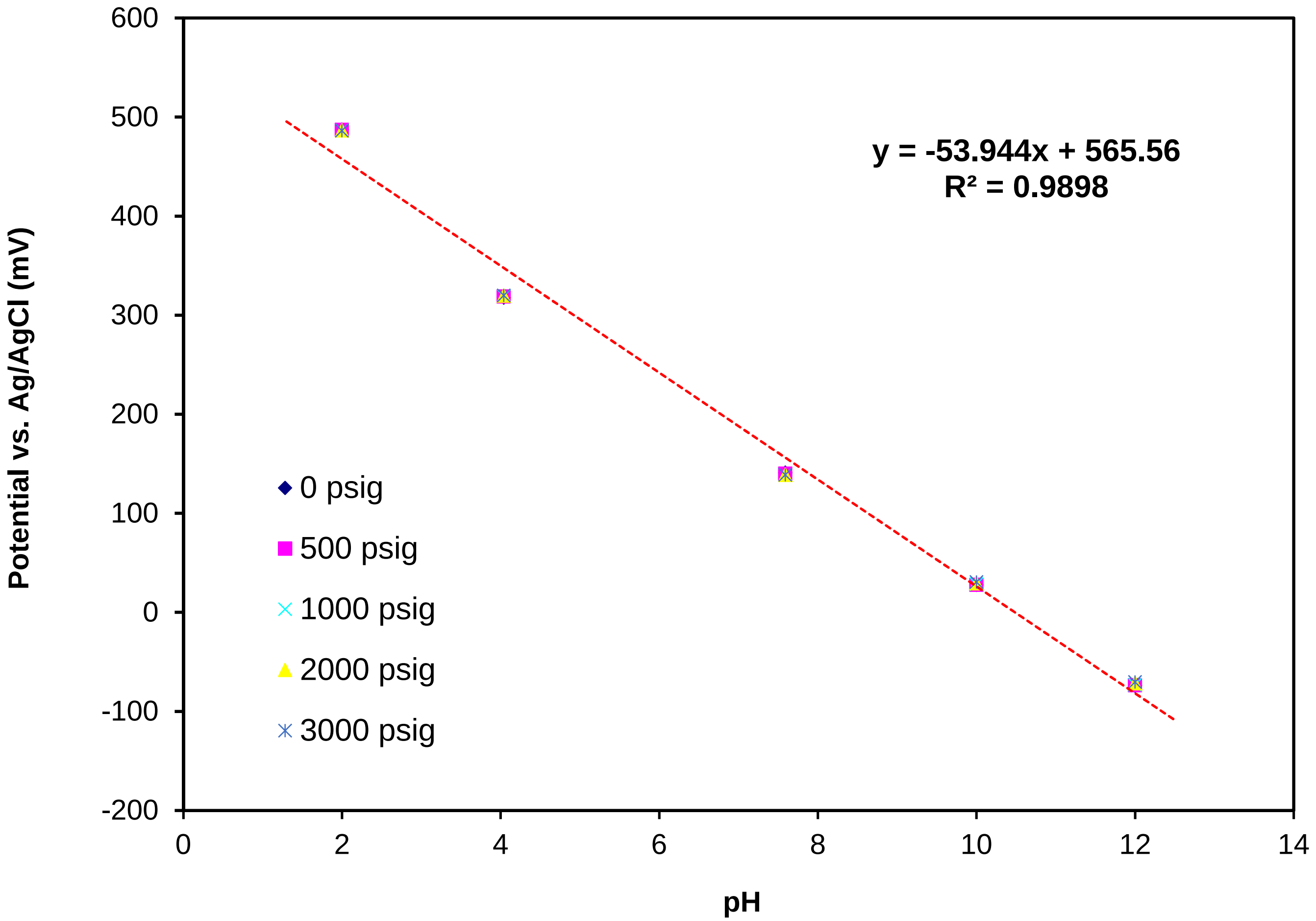

Figure 21. Sensitivity of pH sensor under different pressures.

Reducibility of Iridium oxide electrode

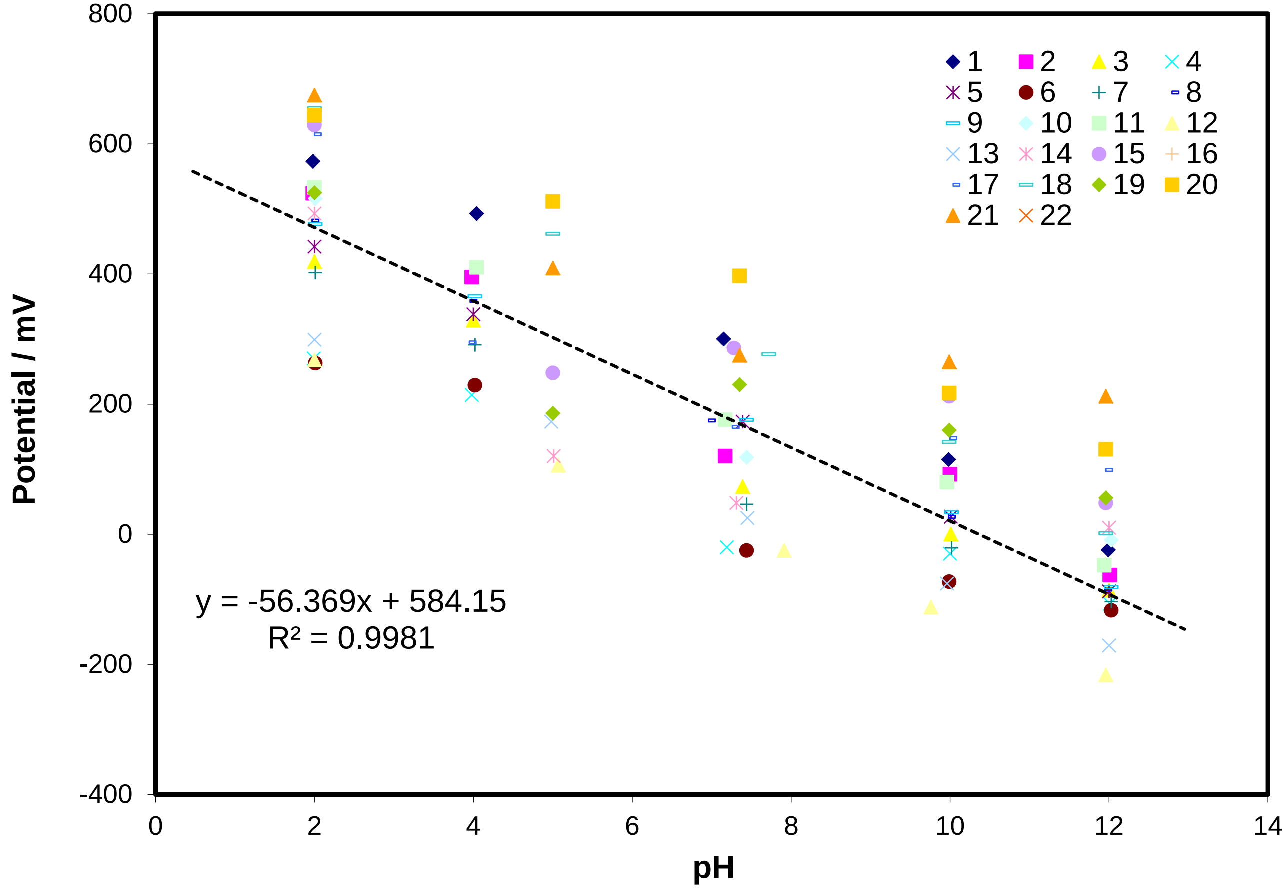

Figure 22. Potential response measurements for 22 iridium oxide film electrodes prepared under the same condition.

Stability of Iridium oxide electrode

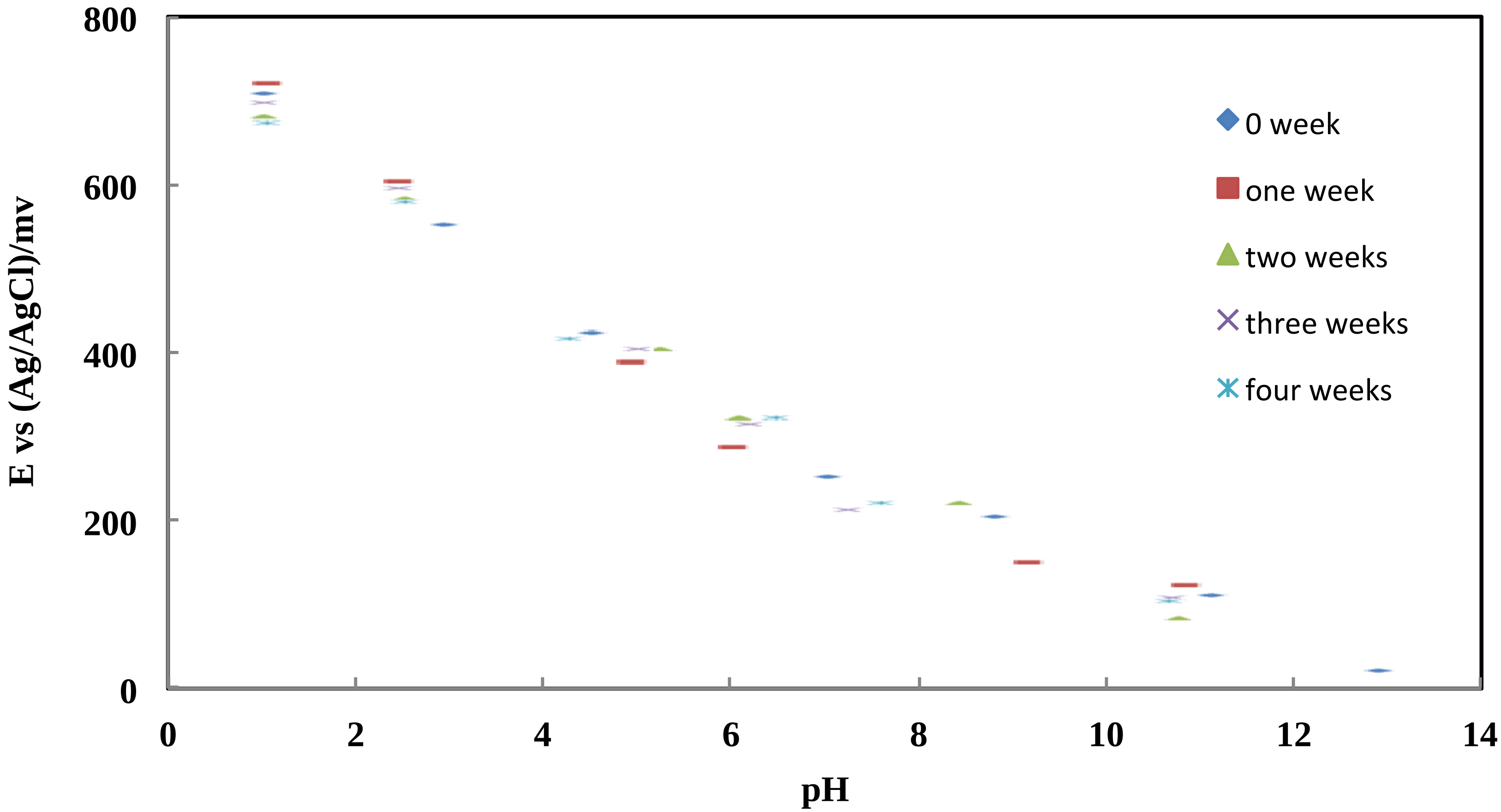

Figure 23. Long-term stability of the IrOx pH electrode in pH buffer solutions.

Current Work

Task 3.0 (1 year) Fabricate downhole CO_2 sensor and test the sensor at high pressure.

- Subtask 2.1 Construct downhole CO_2 sensor
- Subtask 2.2 Test the performance of the CO_2 sensor
- Subtask 2.3 Evaluate the CO_2 sensor in brine solution and high pressure

CO_2 sensor preparation

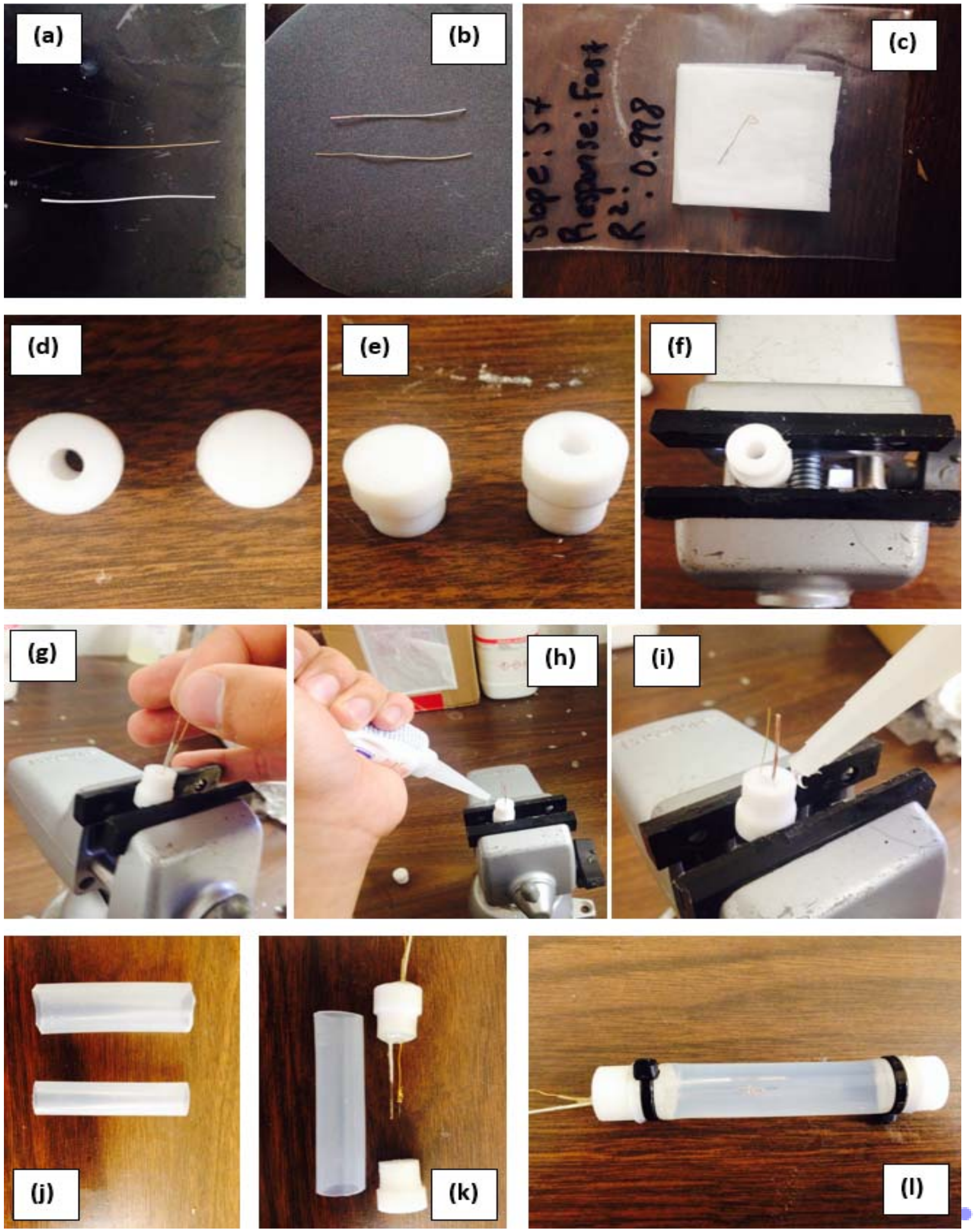

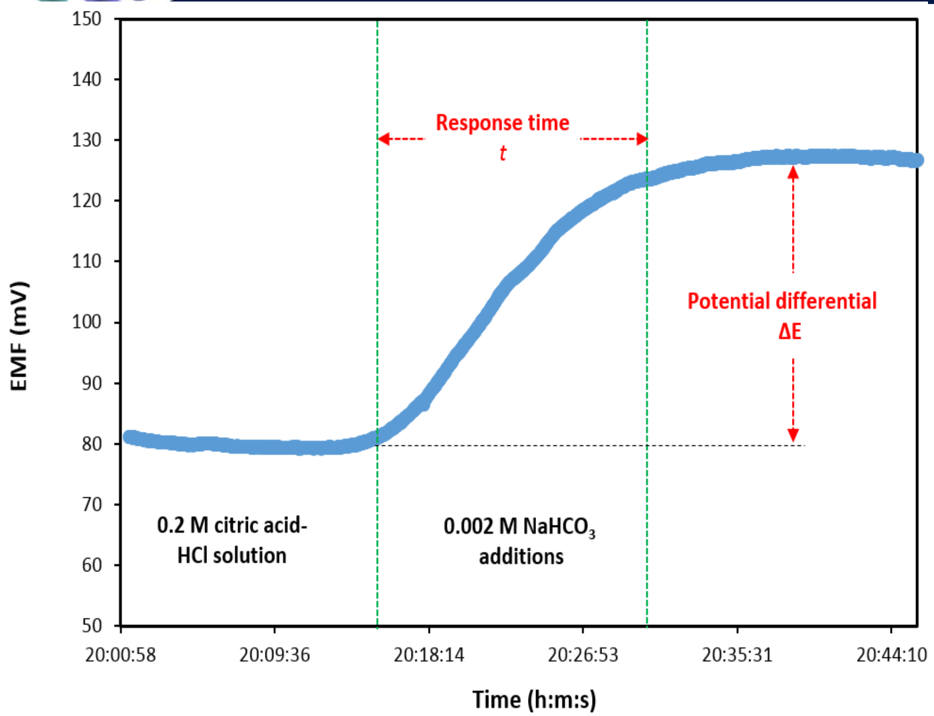

Figure 24. Potential response of the CO_2 sensor as a function of recording time.

Figure 25. Potential different response of the CO_2 .

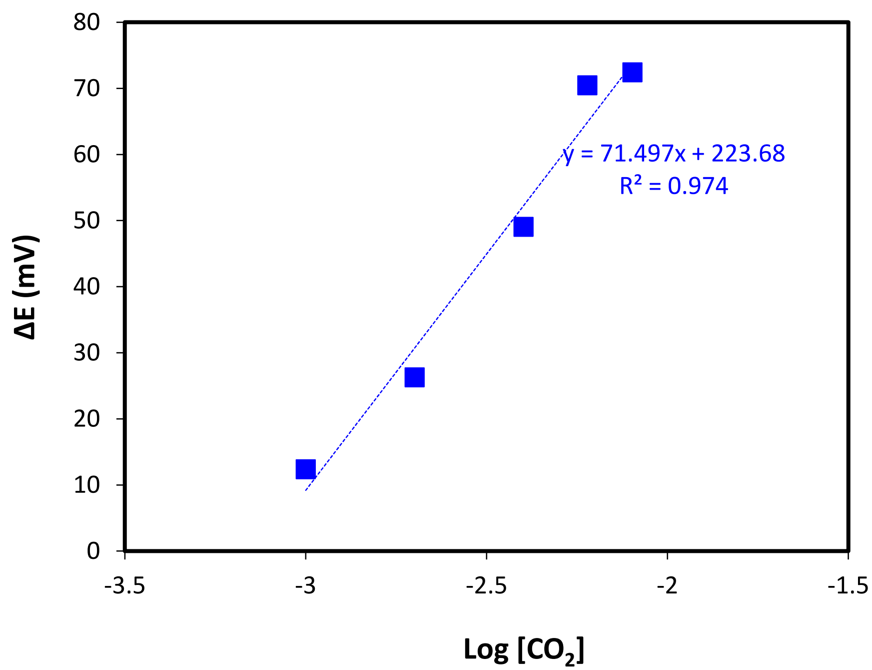

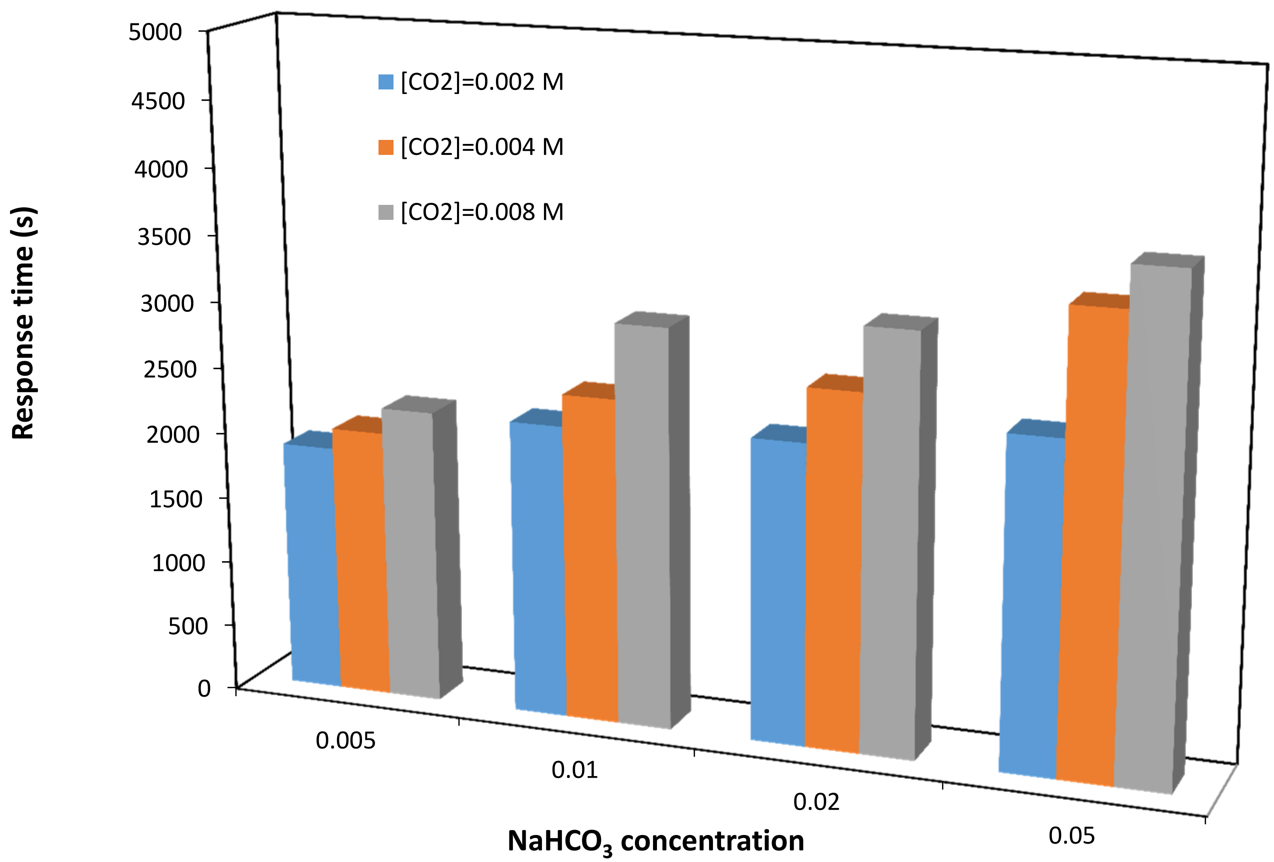

Figure 26. CO_2 sensor response time as a function of $NaHCO_3$.

Table 2 Response Time of CO_2 Sensor in Produced Water

CO_2 concentration (mM)	Log [CO_2]	Response Time (s)
1	-3	2173
2	-2.70	2290
4	-2.40	2475
6	-2.22	2712
8	-2.10	3210

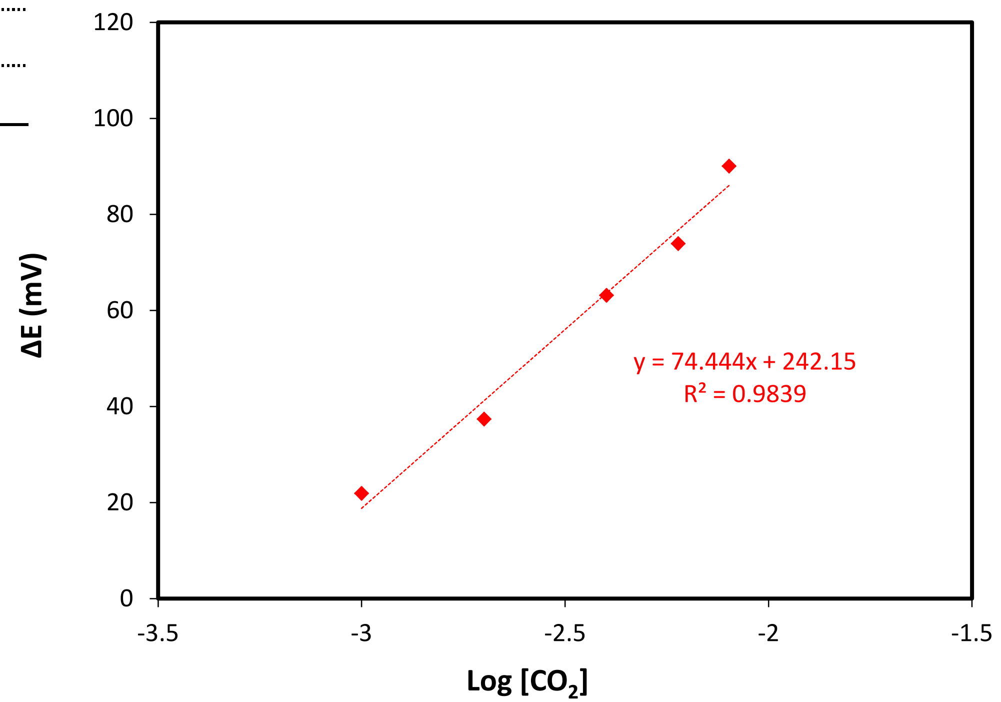

Figure. 27 Potential differential response as a function of the logarithm of the CO_2 concentration in the produced water.

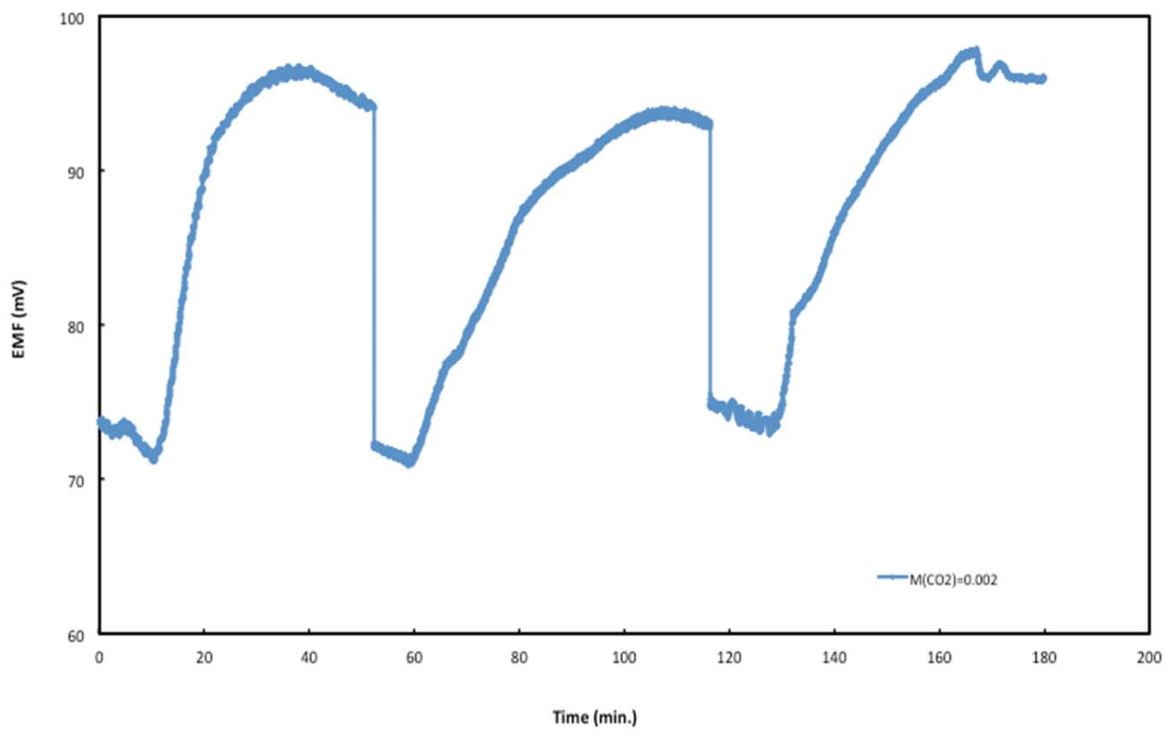

Figure. 28 Reproducibility tests of the CO_2 sensor. (CO_2 concentration = 0.002 M)

Downhole CO_2 sensor fabrication

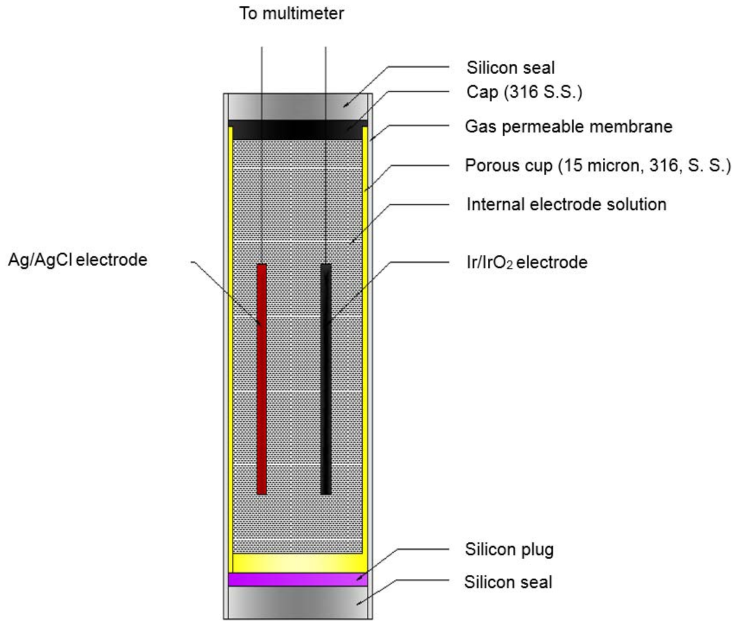

Figure. 29 Schematic design and image of the downhole CO_2 sensor.

CO_2 sensor preparation

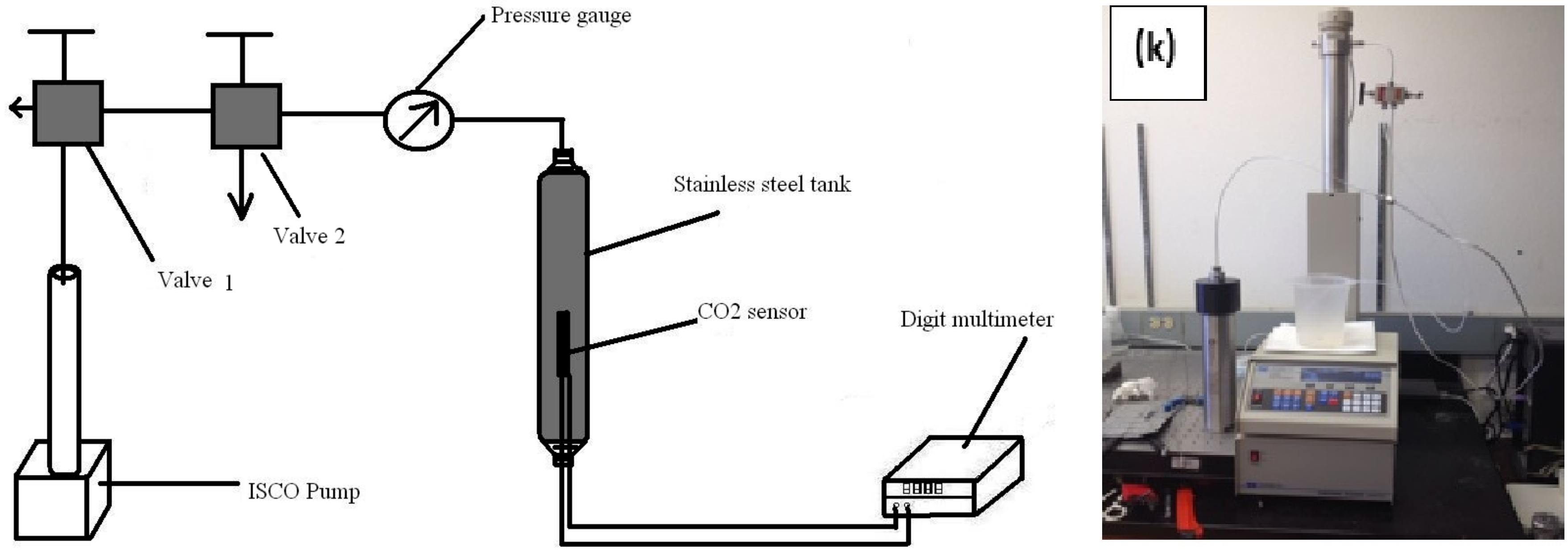

Figure. 30 Schematic diagram of the downhole CO_2 sensor test.

CO_2 sensor preparation

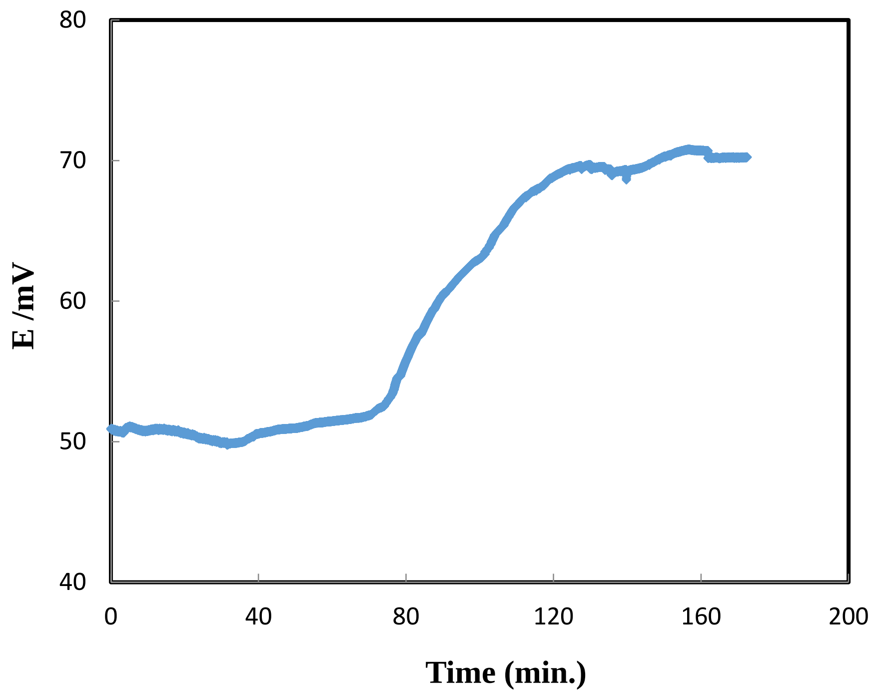

(a)

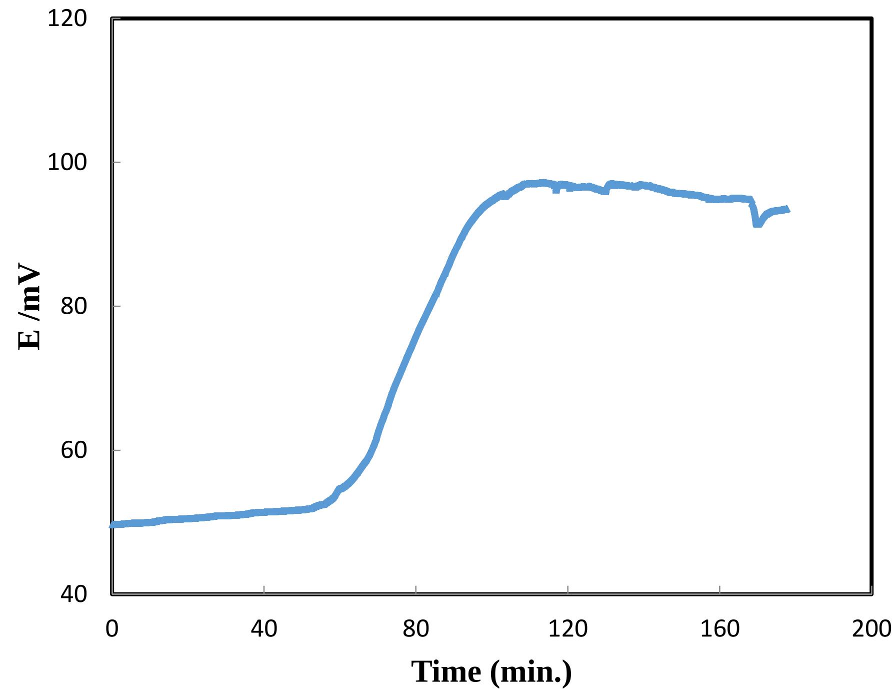

(b)

Figure. 31 Potential response of the CO_2 sensor under 500 psi. CO_2 concentration was: (a) 0.001M; (b) 0.002 M.

Conclusions

- **Iridium oxide electrode was prepared by oxidation of an iridium metal wire in carbonate melt at high temperature. The electrode exhibited a linear response with respect to pH from 1 to 13.**

- **The prepared iridium oxide electrode displayed ions resistance in pH sensing. Different ions such as Na^+, Cl^-, Ca^{2+}, Mg^{2+}, CO_3^{2-}, and SO_4^{2-} were observed to have little effect on the electrode performance.**

- **The prepared iridium oxide electrode could work under high pressure and high salinity of produced water, A smooth linear response was observed when the pH value of the produced water changed from 1 to 13.**

- **An iridium oxide electrode based CO_2 sensor was prepared. The CO_2 sensor could measure the dissolved CO_2 concentration in produced water.**

- **A downhole CO_2 sensor was constructed. The downhole CO_2 sensor could measure the dissolved CO_2 concentration under high pressure.**

Future work

- ***Test the performance of the CO_2 sensor under different pressures.***
- ***Design and conduct CO_2/brine coreflooding tests to evaluate the performance of the CO_2 sensor in the tests.***
- ***Develop a data acquisition system to convert the output of the sensor signal into digital data.***

Acknowledgement

We gratefully acknowledge the support of:

- Department of Energy: DE-FE0009878,
- Petroleum Recovery Research Center at New Mexico Tech.